British Journal of Pharmacology (2009), 156, 1228–1238

0007-1188/09
www.brjpharmacol.org

RESEARCH PAPER

Anti-angiogenic and vascular disrupting effects of C9, a new microtubule-depolymerizing agent

Xuan Ren[1], Mei Dai[1], Li-Ping Lin[1], Pui-Kai Li[2] and Jian Ding[1]

[1]*Division of Anti-tumor Pharmacology, State Key Laboratory of Drug Research, Shanghai Institute of Materia Medica, Chinese Academy of Sciences, Shanghai, China, and* [2]*Division of Medicinal Chemistry and Pharmacognosy, College of Pharmacy, The Ohio State University Columbus, Columbus, OH, USA*

Background and purpose: The critical role of blood supply in the growth of solid tumours makes blood vessels an ideal target for anti-tumour drug discovery. The anti-angiogenic and vascular disrupting activities of C9, a newly synthesized microtubule-depolymerizing agent, were investigated with several *in vitro* and *in vivo* models. Possible mechanisms involved in its activity were also assessed.
Experimental approach: Microtubule-depolymerizing actions were assessed by surface plasmon resonance binding, competitive inhibition and cytoskeleton immunofluorescence. Anti-angiogenic and vascular disrupting activities were tested on proliferation, migration, tube formation with human umbilical vein endothelial cells, and in rat aortic ring, chick chorioallantoic membrane and Matrigel plug assays. Western blots and Rho activation assays were employed to examine the role of Raf-MEK-ERK (mitogen-activated ERK kinase, extracellular signal-regulated kinase) and Rho/Rho kinase signalling.
Key results: C9 inhibited proliferation, migration and tube formation of endothelial cells and inhibited angiogenesis in aortic ring and chick chorioallantoic membrane assays. C9 induced disassembly of microtubules in endothelial cells and down-regulated Raf-MEK-ERK signalling activated by pro-angiogenic factors. In addition, C9 disrupted capillary-like networks and newly formed vessels *in vitro* and rapidly decreased perfusion of neovasculature *in vivo*. Endothelial cell contraction and membrane blebbing induced by C9 in neovasculature was dependent on the Rho/Rho kinase pathway.
Conclusions and implications: Anti-angiogenic and vascular disruption by C9 was associated with changes in morphology and function of endothelial cells, involving the Raf-MEK-ERK and Rho/Rho kinase signalling pathways. These findings strongly suggest that C9 is a new microtubule-binding agent that could effectively target tumour vasculature.
British Journal of Pharmacology (2009) **156**, 1228–1238; doi:10.1111/j.1476-5381.2009.00112.x; published online 19 March 2009

Keywords: C9; anti-angiogenesis; vascular disrupting effect; microtubule; Raf-MEK-ERK signalling pathway

Abbreviations: bFGF, basic fibroblast growth factor; CAM, chick chorioallantoic membrane; ERK, extracellular signal-regulated kinase; FGFR1, FGF receptor 1; GAPDH, glyceraldehyde-3-phosphate dehydrogenase; KDR, receptor for vascular endothelial growth factor; MEK, mitogen-activated ERK kinase; MLC2, myosin light chain2; MTT, 3-(4,5-dimethylthiazol-2-yl)-2,5-diphenyl-tetrazalium bromide; VEGF, vascular endothelial growth factor

Introduction

Functional blood vessels provide oxygen and nutrients to solid tumours and serve as the route for metastatic spread, making tumour vasculature an attractive target for anti-tumour therapy (Ferrara and Kerbel, 2005). Two main strategies have been used to target tumour vasculature: anti-angiogenic and vascular disrupting therapies(Denekamp, 1993; Folkman, 1995).

Correspondence: Jian Ding, Division of Anti-tumor Pharmacology, State Key Laboratory of Drug Research, Shanghai Institute of Materia Medica, Chinese Academy of Sciences, 555 Zu Chong Zhi Road, Zhangjiang Hi-Tech Park, Shanghai 201203, China. E-mail: jding@mail.shcnc.ac.cn
Received 30 June 2008; revised 16 October 2008; accepted 4 November 2008

Anti-angiogenic therapy has been thought to be an important component for cancer treatment since Judah Folkman first addressed the concept in 1971 (Folkman, 1971). Bevacizumab (Avastin), a monoclonal antibody against vascular endothelial growth factor (VEGF) was the first angiogenesis inhibitor approved by Food and Drug Administration. Nine other angiogenesis inhibitors have subsequently been approved or used in different countries (Folkman, 2007). Although these anti-angiogenic drugs are active in cancer treatment, as single agents or in combination with other drugs, they have minimal effects on existing tumour blood vessels within well-established tumours and have had limited effects on large tumours (Bergers *et al.*, 1999; Bergers *et al.*, 2003).

Vascular disrupting therapy using vascular disrupting agents (VDAs) has become attractive as it causes a rapid and

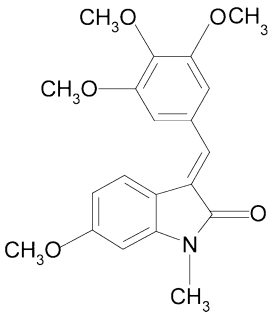

Figure 1 Chemical structure of C9.

selective shutdown of the established tumour vasculature by disrupting the tumour endothelium (Thorpe, 2004). Differences in the physiology of immature tumour vasculature versus mature normal vasculature provide an opportunity for the selective disruption of tumour blood flow (Neri and Bicknell, 2005). One of the potential advantages of VDAs is that they can exert greater actions on large experimental tumours than small ones (Landuyt *et al.*, 2000; Siemann and Rojiani, 2005). In addition, VDAs produce central necrosis in experimental tumours, but have no effect on the thin rim of the tumour periphery, where angiogenesis occurs most vigorously.

As such, the development of new compounds with both anti-angiogenic and vascular targeting properties has attracted greater attention (Belleri *et al.*, 2005; Kruczynski *et al.*, 2006). A newly synthesized compound, C9 (Figure 1), was identified during our search for a potential candidate agent with both activities. Preliminary studies with C9 suggested it inhibited microtubule polymerization *in vitro* (Li *et al.*, 2005). The current study aims to investigate the potential anti-angiogenic activity of C9 and to further characterize its anti-vascular properties and mechanisms of action *in vitro* and *in vivo*.

Methods

Cell culture

Human umbilical vein endothelial cells (HUVECs) were isolated as previously described (Jaffe *et al.*, 1973), and presence of von Willebrand factor was confirmed by immunofluorescence staining. HUVECs were cultured (37°C, 5% CO_2) in M199 medium supplemented with 20% heat-inactivated fetal bovine serum (FBS) containing 30 μg·mL^{-1} endothelial cell growth supplement, 10 ng·mL^{-1} epidermal growth factor, 100 units·mL^{-1} penicillin and 100 μg·mL^{-1} streptomycin. Cells at passages 3–7 were used for experiments.

Cell proliferation assay

Human umbilical vein endothelial cells (1.0×10^5 cells·mL^{-1}) were seeded onto 96-well plates, attached overnight and subsequently exposed to different concentrations of C9 (0.03, 0.06, 0.13, 0.25, 0.5, 1.0 and 2.0 μmol·L^{-1}) for 12, 24, 36 or 48 h. Cell proliferation was determined by MTT [3-(4, 5-dimethylthiazol-2-yl)-2,5-diphenyl-tetrazalium bromide] assay (Alley *et al.*, 1988). The inhibition rate of cell proliferation was calculated as: growth inhibition (%) = ($OD_{control}$ − $OD_{treated}$)/$OD_{control}$ × 100%.

Cell cycle assay

Cells (5.0×10^5) were fixed in 70% ice-cold ethanol, centrifuged, washed with phosphate-buffered solution (PBS), centrifuged, resuspended in 1 mL DNA-staining solution (20 μg·mL^{-1} RNase, PBS and 20 μg·mL^{-1} propidium iodide) and incubated (30 min, room temperature, in the dark). Cell samples (at least 1.0×10^5) were then examined by a FACS Calibur analyser. Cell cycle phase analysis was performed by utilizing Modifit software (BD, San Jose, CA, USA).

Cytoskeleton immunofluorescence

Human umbilical vein endothelial cells were seeded on fibronectin-coated chamber slides (10 μg·mL^{-1}) before exposure to C9 (0.5 μmol·L^{-1}, 1 h). Tubulin was visualized with FITC-anti-tubulin monoclonal antibody (Sigma) and F-actin with Alexa Fluor 633 Phalloidin (Molecular Probes, OR, USA). Slides were mounted by using VECTASHIELD (Vector laboratories, CA, USA). Fluorescence images were obtained by using a Lecia TCS confocal microscope (Leica, Deerfield, IL, USA).

Surface plasmon resonance (SPR)-binding assay

Tubulin-binding assays were performed by using an SPR technology-based Biacore 3000 instrument (Biacore AB, Uppsala, Sweden) as described by Li *et al.*, (2007). Briefly, tubulin was covalently immobilized on a CM5 sensor chip (BIAcore), and indicated concentrations of the compound were dissolved in the running buffer. The equilibrium dissociation constant (K_D) was derived by fitting the data by using the 1:1 Langmuir binding model based on BIAevaluation 3.1 software.

Competitive inhibition assay

Colchicine binding to tubulin. The tubulin-colchicine complex was formed by incubating 3 μmol·L^{-1} tubulin with colchicine (30 min, 37°C, excitation 365 nm, emission 435 nm). C9 (0–50 μmol·L^{-1}) or vinblastine (0–50 μmol·L^{-1}) was then added to the preformed tubulin-colchicine complex (60 min, 37°C), and fluorescence was measured by using a Hitachi F-2500 spectrofluorimeter (n = 3).

Vinblastine binding to tubulin. Binding of the fluorescent conjugate of vinblastine (BODIPY FL-vinblastine; Molecular probes Inc., Eugene, OR, USA) to tubulin will increase fluorescence at 490 nm excitation wavelength (Gupta *et al.*, 2004). Tubulin (3 μmol·L^{-1}) was incubated with various concentrations of C9 (45 min, 37°C) or vinblastine, then incubated with BODIPY FL-vinblastine (2 μmol·L^{-1}, 20 min, 37°C). Data were analysed by a Hitachi F-4500 fluorimeter.

Cell migration assay

Human umbilical vein endothelial cell migration was determined in a transwell Boyden chamber (Costar, MA, USA)

(Osusky *et al.*, 2004). Briefly, cell suspensions (5×10^5 cells·mL^{-1}) with different concentrations of C9 (0.25, 0.5, 1.0 and 2.0 μmol·L^{-1}) or control was added to the upper compartment of the chamber. The lower compartment contained 20% FBS M199 medium and the same concentrations of C9 or control. After incubation (8 h, 37°C), the inhibition of migration was calculated thus: inhibition of migration = $[1 - (A_{compound} - A_{blank})/(A_{control} - A_{blank})] \times 100\%$.

Tube formation assay

Matrigel (55 μL·well^{-1}) was used to coat 96-well plates, allowed to solidify (37°C, 1 h) (Soeda *et al.*, 2000), prior to seeding with HUVECs (1×10^5 cells·mL^{-1}) that were then cultured (37°C, 6 h) in M199 medium with 20% FBS containing C9 (0.25, 0.5, 1.0 and 2.0 μmol·L^{-1}) or control.

For investigation of neovessel disruption, HUVECs were seeded on Matrigel (9.3 mg·mL^{-1}) and left to align for 24 h (Kruczynski *et al.*, 2006). The formed capillary-like structures or cords were exposed to C9 (0.5 μmol·L^{-1}) then examined with an inverted phase contrast microscope (DP70, Olympus, Japan). The number of the tubes was quantified from five random fields (Ashton *et al.*, 1999). The inhibition of tube formation was calculated thus: inhibition of tube formation = $[1 - (tubes_{C9}/tubes_{control})] \times 100\%$.

Aortic ring assay

All animal procedures and experiments complied with the ethical Guidelines for the care and use of animals and were approved by the Institute animal reviews boards of Shanghai Institute of Materia Medica, Chinese Academy of Sciences. Aortic rings obtained from 6-week-old Sprague–Dawley rats (Nicosia and Ottinetti, 1990; Belleri *et al.*, 2005) were embedded with 30 μL Matrigel, incubated with M199 medium, with or without 10% FBS, and various concentrations of C9 (0.5, 1.0 and 2.0 μmol·L^{-1}), then photographed on day 7 with an inverted phase contrast microscope (DP70, Olympus, Japan). The degree of endothelial cell sprouting from aorta samples was analysed with computer image analysis (Image pro-plus 4.5; Media Cybernetics, LP), with inhibition rate calculated as: inhibition rate of sprouting areas of the aortic ring = $[1 - (\text{sprouting areas}_{C9}/\text{sprouting areas}_{control})] \times 100\%$.

Rings cultured for 7 days were used in disruption assays of neo-formed vessels (Belleri *et al.*, 2005). Neovessels were photographed at different time points after treatment with C9 (0.5 μmol·L^{-1}, 24 h).

Chick chorioallantoic membrane (CAM) assay

Fertilized chicken eggs were incubated (7 days) in a humidified egg incubator Roll-X base (Lyon Electric Company, CA, USA) (Ribatti *et al.*, 2000). The chorioallantoic membrane (CAM) was treated with various concentrations of C9 or 0.01% dimethyl sulphoxide (v/v) continuously for 48 h, then evaluated and recorded by stereomicroscopic photography (MS5, Leica, Switzerland). Angiogenesis was quantified by counting the number of blood vessel branch points in each photograph under the coverslips; at least 10 viable embryos were tested for each treatment. The CAM inhibition rate was measured as: inhibition of CAM = $[1 - (branches_{C9}/branches_{control})] \times 100\%$.

In vivo *Matrigel plug assay*

A Matrigel plug assay was employed as previously described (Micheletti *et al.*, 2003), with some modifications. Briefly, basic fibroblast growth factor (bFGF; 100 ng per pellet) was embedded in a Matrigel pellet (0.5 mL) and s.c. injected into C57BL/6N mice. On day 7, when functional vessels were formed and evident in the plug, C9 (200 mg·kg^{-1}, i.p.) was injected into mice for 1 or 3 h before necropsy. Mice were injected i.v. with FITC-conjugated dextran (100 μL, Sigma, St. Louis, MO, USA) 1 h before necropsy. The Matrigel was removed and FITC-positive vessels were analysed by fluorescence microscopy (BX51, Olympus, Japan) at 488 nm.

Western blot analysis

Human umbilical vein endothelial cells (5×10^6 cells·mL^{-1}) were treated, and cell lysates were prepared as previously described (Tan *et al.*, 2004). Equal amounts of protein were separated on SDS-PAGE gels and transferred to nitrocellulose membranes, incubated (overnight, 4°C) with primary antibodies followed by horseradish peroxidase-conjugated secondary antibodies (1 : 2000). Detection was performed by using ECL Plus Western Blotting Detection System.

Rho activation assay

Rho activation was analysed by using Rho assay kits (Upstate Biotechnology). Briefly, HUVECs grown in 100 mm diameter dishes were serum-starved (2 h) followed by pretreatment with vehicle, Y27632 (10 μmol·L^{-1}) or taxol (0.2 μmol·L^{-1}) for 30 min, then exposed to C9 (0.5 μmol·L^{-1}, 1 h). Cells were then rinsed with ice-cold PBS buffer and lysed (lysis buffer, 500 μL per plate), following the manufacturer's protocol. Cell lysates were clarified by centrifugation (14 000× *g*, 4°C, 5 min), supernatants incubated with glutathione S-transferase (GST)-Rhotekin-Rho-binding domain (RBD) (GST-RBD) beads (4°C, 45 min), and washed three times with the wash buffer. Bound Rho proteins were detected by Western blotting using a monoclonal antibody against Rho. RBD-bound Rho was normalized to the total amount of Rho in cell lysates for comparison of Rho activity in different samples (Ren *et al.*, 1999).

Statistical analysis

All results are expressed as mean ± SD. Statistical significance was assessed by two-tailed Student's *t*-test.

Materials

C9, (2H-Indol-2-one, 1, 3-dihydro-6-methoxy-1-methyl-3-[(3, 4, 5-trimethoxyphenyl) methylene]-, (3E)-(9CI) (Figure 1), was prepared with commercially available 6-methoxy-2-indolinone as previously described (Li *et al.*, 2005; Pandit

et al., 2006). The stock solution (10^{-2} mol·L^{-1}) was made in dimethyl sulphoxide. Type I collagenases, endothelial cell growth supplement, epidermal growth factor, MTT, DAPI, propidium iodide, tubulin, taxol, Y27632, colchicine and antibodies to von Willebrand factor were purchased from Sigma Aldrich (St. Louis, MO, USA); M199 medium and FBS from Gibco (Grand Island, NY, USA); VEGF and bFGF from R&D systems (Minneapolis, MN, USA); Matrigel from BD Biosciences (San Jose, CA, USA); antibodies to phosphorylated form of the VEGF receptor (KDR), FGF receptor (FGFR)1, c-Raf, extracellular signal-regulated kinase (ERK), mitogen-activated ERK kinase (MEK), Akt and myosin light chain2 (MLC2) from Cell Signaling Technology (Danvers, MA, USA); antibody to GAPDH (glyceraldehyde-3-phosphate dehydrogenase) from KangChen Bio-tech (Shanghai); secondary antibodies from Calbiochem (San Diego, CA, USA), and ECL Plus Western Blotting Detection System was purchased from GE Healthcare (UK).

Results

C9 as a tubulin-depolymerizing agent

C9 disrupts the cytoskeleton and changes the morphology of endothelial cells. C9 disrupted tubulin polymerization with an IC_{50} of approximately 13 μmol·L^{-1} (Pandit *et al.*, 2006). The effects of C9 on microtubule and F-actin cytoskeleton organization were examined by immunofluorescence. As shown in Figure 2A, C9 led to a dramatic disruption of the HUVEC cytoskeleton, producing a diffuse microtubule network and an increase in actin stress fibres and membrane blebbing. At the same time, cell morphology was significantly changed, with rounded and retracted shape following exposure to C9 (see later).

C9 induces G2/M phase arrest. Given the correlation between G2/M phase arrest and cytoskeletal dynamics, we next investigated the effect of C9 on the cell cycle. Our data showed that treatment with C9 (24 h) induced a dose-dependent reduction in the proportion of cells in G0/G1, with a concomitant accumulation of cells arrested in G2/M (Table 1).

C9 binds to the colchicine-binding site of tubulin. Most microtubule-targeting agents interact with either the *Vinca* alkaloid (Downing, 2000) or the colchicine site (Ravelli *et al.*, 2004) of tubulin. We examined whether C9 exerted its activity through binding to either of these two sites. Colchicine is weakly fluorescent in aqueous solution but becomes strongly fluorescent upon binding to tubulin (Hastie, 1991). As expected, no decrease in fluorescence was noted following vinblastine, which is known to bind to tubulin at the *Vinca* alkaloid site. Conversely, 5–50 μmol·L^{-1} C9 competed with colchicine to bind to tubulin, releasing colchicine from the complexes with consequent decrease of fluorescence (75.6%

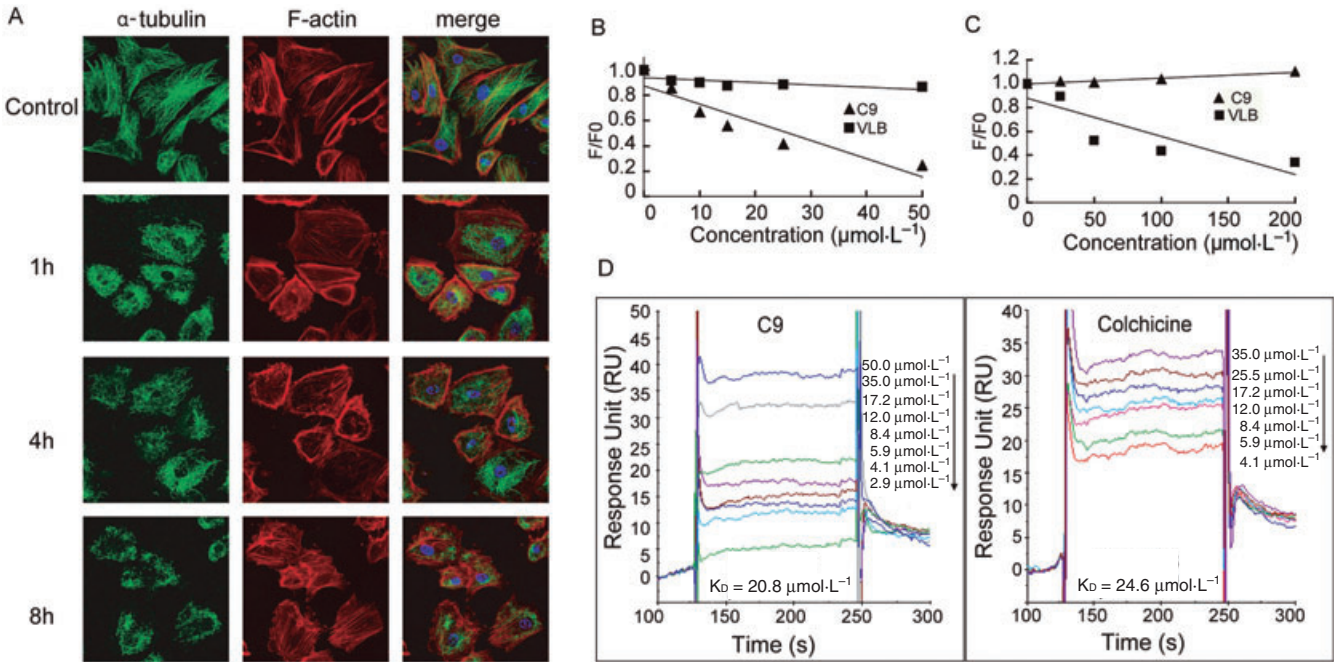

Figure 2 C9 is a microtubule-binding agent. (A) Effects of C9 on the endothelial cell cytoskeleton. Human umbilical vein endothelial cells were seeded onto coverslips coated with fibronectin and incubated overnight prior to treatment (1, 4 and 8 h, with or without 0.5 μmol·L^{-1} C9). Cells were then fixed and stained for microtubules (green) and F-actin (red); fluorescence images were viewed by using a Leica TCS confocal microscope (43×). (B) Effects of C9 on the colchicine-binding site. Tubulin (3 μmol·L^{-1}) was incubated with colchicine to form tubulin-colchicine binding complexes prior to treatment (37°C, 60 min) with C9 (5, 10, 15, 25 and 50 μmol·L^{-1}) or vinblastine (VLB; 5, 10, 15, 25 and 50 μmol·L^{-1}). (C) Effects of C9 on the *Vinca* alkaloid site. Tubulin (3 μmol·L^{-1}) was incubated (37°C, 45 min) with various concentrations of C9 (25, 50, 100 and 200 μmol·L^{-1}) or vinblastine (VLB; 25, 50, 100 and 200 μmol·L^{-1}) prior to treatment with BODIPY FL-vinblastine (20 min, 37°C). (D) C9 or colchicine tubulin-binding affinity by surface plasmon resonance assay. C9 (2.9, 4.1, 5.9, 8.4, 12.0, 17.2, 35.0 and 50.0 μmol·L^{-1}) or colchicine (4.1, 5.9, 8.4, 12.0, 17.2, 24.5 and 35.0 μmol·L^{-1}) were prepared as an analyte and then injected into a Biacore 3000 system following tubulin immobilization on the chip.

Table 1 C9 blocks the cell cycle in human umbilical vein endothelial cells at the G2/M phase

	C9 (μmol·L⁻¹)				
	0	*0.25*	*0.5*	*1.0*	*2.0*
G1 phase (%)	67.4 ± 6.1	66.3 ± 4.4	54.6 ± 5.2	51.1 ± 1.5	48.3 ± 11.4
S phase (%)	17.1 ± 1.5	11.3 ± 9.4	10.6 ± 9.2	11.7 ± 10.3	*4.8 ± 6.9
G2 phase (%)	15.5 ± 6.2	22.4 ± 5.1	34.8 ± 12.3	*37.2 ± 9.5	*46.9 ± 9.1

Data shown in the table are percentage of cells in the phases of the cell cycle indicated, as measured by FACS (see *Methods*). Incubation with increasing concentrations of C9 decreased the proportion of cells in the S phase and increased that in the G2 phase.
*Significantly different from corresponding value in control cultures (C9 at 0 μmol·L^{-1}); Student's *t*-test. At least 10^5 cells were assessed from three separate cultures.

at 50 μmol·L^{-1}), suggesting that C9 competed for the same tubulin-binding site as colchicine (Figure 2B).

We next investigated whether C9 inhibited BODIPY FL-vinblastine binding to tubulin using a BODIPY FL-vinblastine competition-binding assay. While we observed no inhibitory effect of C9, the positive control vinblastine (50 μmol·L^{-1}) decreased the fluorescence by 47.8%. These results suggested that C9 binds with tubulin through the colchicine site and not the vinblastine-binding site (Figure 2C).

C9 exhibits high binding affinity for tubulin. We subsequently investigated the binding affinity of C9 for tubulin. SPR sensor kinetic analysis data demonstrated that the C9 equilibrium dissociation constant K_D was 20.8 μmol·L^{-1}, compared with 24.6 μmol·L^{-1} for colchicine, suggesting C9 and colchicine have similar binding affinities for tubulin (Figure 2D).

Anti-angiogenic activity of C9

C9 inhibits endothelial cell proliferation. Angiogenesis is a complex process that includes the proliferation, migration and tube formation of endothelial cells. We first tested the inhibitory effect of C9 on endothelial cell proliferation by MTT assay. As shown in Figure 3A, C9 treatment (48 h) had little effect on cell growth at 0.03, 0.06, 0.1, 0.2 and 0.5 μmol·L^{-1} and exhibited slight growth inhibition at 1.0 and 2.0 μmol·L^{-1} (11.8% and 34.9% respectively). Therefore, concentrations below 2 μmol·L^{-1} C9 were used to assess the anti-angiogenic effects in HUVECs.

C9 blocks migration of endothelial cells. Endothelial cell migration, which occurs through chemotaxis, is necessary for angiogenesis. As shown in Figure 3B, treatment with 0.25–2.0 μmol·L^{-1} C9 (8 h, a and b) significantly reduced the number of migrating cells in a concentration-dependent manner, compared with controls. When endothelial cells were exposed to 0.5 μmol·L^{-1} C9 for 8 h, only a marginal proliferation inhibitory effect was observed (9.9% ± 2.4), but the migration of endothelial cells was strongly inhibited, suggesting that inhibition of migration by C9 did not result from its cytotoxity.

C9 impairs capillary tube formation. We further evaluated the effects of C9 on the formation of functional tubes utilizing HUVECs plated on a Matrigel substratum. In the control group, stimulation with 20% FBS resulted in the rapid alignment of HUVECs and formation of tube-like structures, within 6 h (Figure 3B, c). C9 suppressed FBS-stimulated tube formation in a concentration-dependent manner, suggesting C9 interfered with the ability of HUVECs to form capillary-like tubes *in vitro*, one of the important traits of endothelial cells.

C9 decreased vessel sprouting from aortic rings and reduced newly formed blood vessels embedded in Matrigel. The effects of C9 on microvessel sprouting from vascular tissues were tested by using an *ex vivo* rat aortic ring assay, which mimics several processes in angiogenesis, including endothelial cell proliferation, migration and tube formation. Microvessels were observed in the control group on days 2–3, with the number and length of microvessels increasing with prolonged culture time (Figure 3B, e and f). Treatment with C9 resulted in a decrease of capillary sprouting in a dose-dependent manner, with a microvessel growth inhibition of almost 60% noted after exposure to 0.5 μmol·L^{-1} C9 for 7 days.

C9 reduces neovascularization in CAM assay. CAM assays were used to examine the effects of C9 *in vivo* as they provide a unique model to investigate the process of new blood vessel formation and effects of anti-angiogenic agents. Compared with the control group, neovascularization of CAM treated with C9 (5 nmol per egg) was dramatically decreased, an inhibitory effect that was also concentration-dependent (Figure 3B, g and h). These results suggested that C9 inhibited angiogenesis *in vitro*, *ex vivo* and *in vivo*, in a concentration-dependent manner.

C9 anti-angiogenic activity is mediated through down-regulation of Raf-MEK-ERK signalling molecules. We further examined the mechanisms of anti-angiogenic activity of C9 treatment. VEGF and bFGF stimulate the proliferation, migration and differentiation of endothelial cells via binding to their receptors and receptor activation. We evaluated the effects of C9 on endothelial cell-specific receptors for VEGF (KDR) or bFGF (FGFR1) and their downstream signalling pathways. HUVECs were exposed to various concentrations of C9 for 2 h after 24 h serum starvation and subsequently stimulated (10 min) with VEGF (50 ng·mL^{-1}) or bFGF (25 ng·mL^{-1}). The phosphorylation of KDR and FGFR1 and overall KDR and FGFR1 expression levels in cells (Figure 4A,B) were not affected by pretreatment with C9 (1 μmol·L^{-1} and 2 μmol·L^{-1}). However, phosphorylation of downstream molecules Raf, MEK and

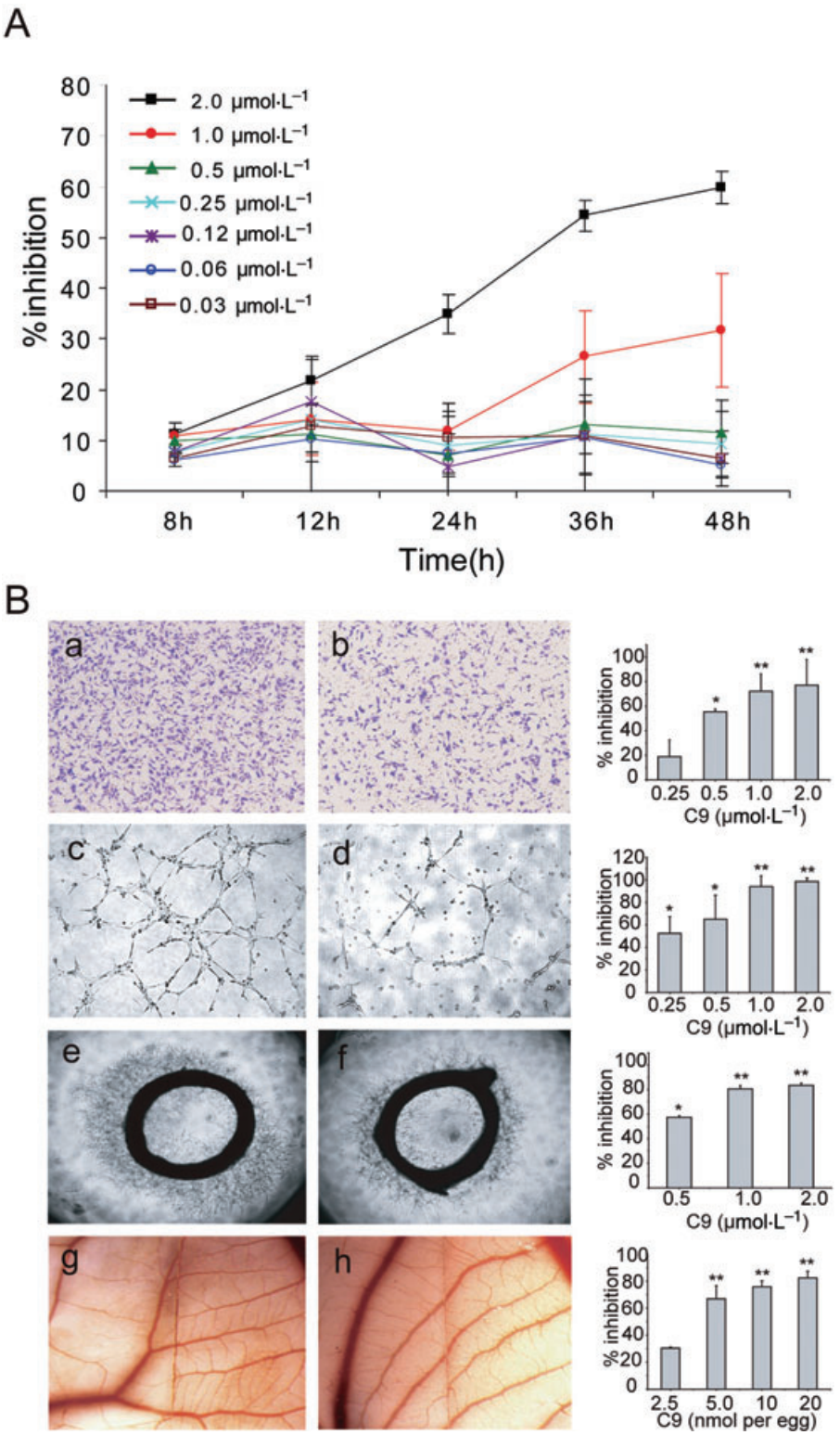

Figure 3 C9 inhibited angiogenesis. (A) C9 inhibited endothelial cell proliferation. Human umbilical vein endothelial cells were incubated overnight then exposed to different concentrations of C9 (0.03, 0.06, 0.12, 0.25, 0.5, 1.0 and 2.0 μmol·L^{-1}) and cultured for 8, 12, 24, 36 and 48 h. Inhibition of proliferation was measured by the MTT [3-(4,5-dimethylthiazol-2-yl)-2,5-diphenyl-tetrazalium bromide] assay. (B) Inhibitory effect of C9 on cell migration, tube formation, aortic ring and chick chorioallantoic membrane assays. Representative images and summary data (bar graphs on right hand side) showing inhibition of migration (a and b), tube formation (c and d), angiogenesis in aortic ring (e and f) and chick chorioallantoic membrane assays (g and h). Cells were treated with vehicle (a, c, e and g) or 0.5 μmol·L^{-1} C9 (b, d and f) or 5 nmol per egg C9 (h) (see *Methods*); magnification: 100× (a, b, c and d), 40× (e and f), 1.6× (g and h). Results are expressed as mean ± SD; $n = 3$; *$P < 0.01$ versus control, **$P < 0.005$ versus control.

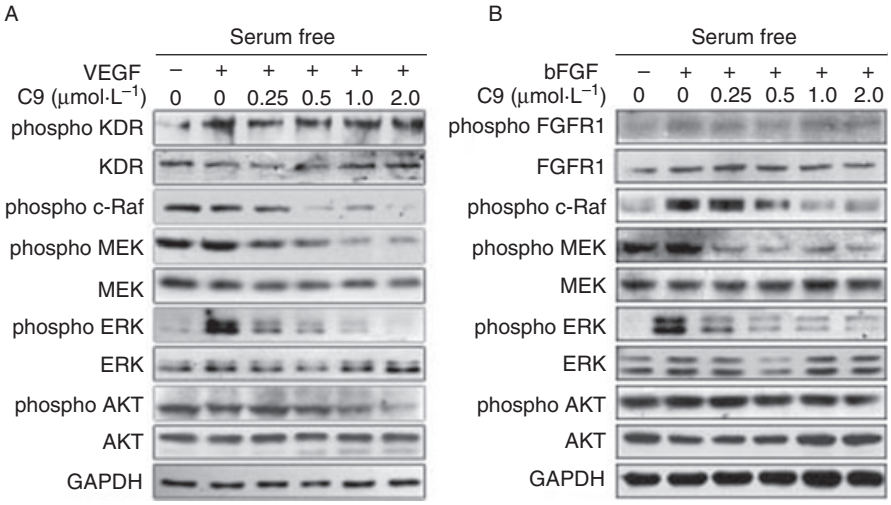

Figure 4 C9 down-regulated the Raf-MEK-ERK signalling pathway induced by VEGF and bFGF. Serum-starved cells were treated with different concentrations of C9 for 2 h, followed by the addition of 50 ng·mL^{-1} VEGF or 25 ng·mL^{-1} bFGF (10 min), then assayed by Western blotting (n = 3). bFGF, basic fibroblast growth factor; ERK, extracellular signal-regulated kinase; FGFR1, FGF receptor 1; GAPDH, glyceraldehyde-3-phosphate dehydrogenase; KDR, receptor for vascular endothelial growth factor; MEK, mitogen-activated ERK kinase; VEGF, vascular endothelial growth factor.

ERK1/2 was down-regulated in a concentration-dependent manner (0.25, 0.5, 1.0 and 2.0 μmol·L^{-1}). Interestingly, effects on Akt phosphorylation were only noted at high concentrations (2 μmol·L^{-1}). In all cases, total steady state protein levels remained unchanged. These results suggested that reduction by C9 of phosphorylation in the Raf-MEK-ERK signalling pathway, contributed to the anti-angiogenic effects of this compound.

Vascular disrupting effect of C9

We then tested the vascular targeting effects of C9 utilizing *in vitro*, *ex vivo* and *in vivo* models. HUVECs seeded on Matrigel will form a network, which is typically completed within 24 h (Figure 5A). The addition of C9 (3 h) to these newly formed capillary-like structures disrupted the network, after 3 h and this effect increased over the following 9 h (Figure 5A).

In the aortic ring assay, vessels grow continuously and become bushy by day 7. Time course experiments showed that formed vessels were cleaved following treatment with C9 (0.5 μmol·L^{-1}) in a time-dependent manner (Figure 5B).

We further evaluated the vascular disruptive effects of C9 *in vivo* using Matrigel plug assays, in which a pellet of Martigel containing bFGF was implanted s.c. After 7 days of implantation, fluorescent dextran was injected i.v. to assess the function of the newly formed vasculature. As shown in Figure 5C, in the control group, functional blood vessels were perfused by FITC-dextran. However, C9 treatment (1 h) resulted in a rapid reduction of vessels and the perfusion of FITC-dextran almost disappeared after 3 h of treatment. Taken together, these data indicated that C9 showed not only anti-angiogenic, but also vascular-disrupting activities *in vitro* and *in vivo*.

Morphological changes in HUVECs induced by C9

Cell morphology is an important indicator of endothelial cell behaviour (Schmidt *et al*., 2006). We found that cells became rounded and retracted, accompanied by membrane blebbing following treatment of C9 (Figure 6A). Taxol, a microtubule-polymerizing agent, can reverse the effect of microtubule-depolymerizing agents (Taraboletti *et al*., 2005). Pretreatment with taxol resulted in the rounded or retracted cells becoming extended. In addition, taxol pretreatment attenuated the disruptive effects of C9 on existing HUVEC networks in Matrigel, with inhibition decreasing markedly (Figure 6B).

The Rho/Rho kinase signalling pathway is a critical regulator of the cytoskeleton and of cell behaviour. We therefore examined the effect of the Rho kinase inhibitor Y27632 on C9-driven events. We found that Y27632 attenuated cell morphology changes induced by C9. Similarly, pretreatment with Y27632 protected HUVEC networks from disruption by C9, with a striking reduction in inhibition (Figure 6B). C9 was further noted to activate Rho GTPase and induce phosphorylation of MLC2; both of these effects were reversed by pretreatment with Y27632 (Figure 6C).

Discussion

Anticancer therapies focused on tumour vasculature are classified into anti-angiogenic and vascular disrupting therapies, with many successful compounds having been employed clinically. Microtubules, one of the major dynamic and structural cellular components, are essential for cell function and are, consequently, an attractive target not only for cancer chemotherapy, but also as agents targeting tumour vasculature (Jordan and Wilson, 1998). Microtubule-destabilizing agents, such as combretastatin and vinblastine, are also described as VDAs, with observed anti-angiogenic activity, even at low concentrations (Vincent *et al*., 2005). Consistent with this notion, the vascular targeting and anti-angiogenic activity of C9 were clearly observed *in vitro*, but this compound showed limited inhibition of endothelial cell prolifera-

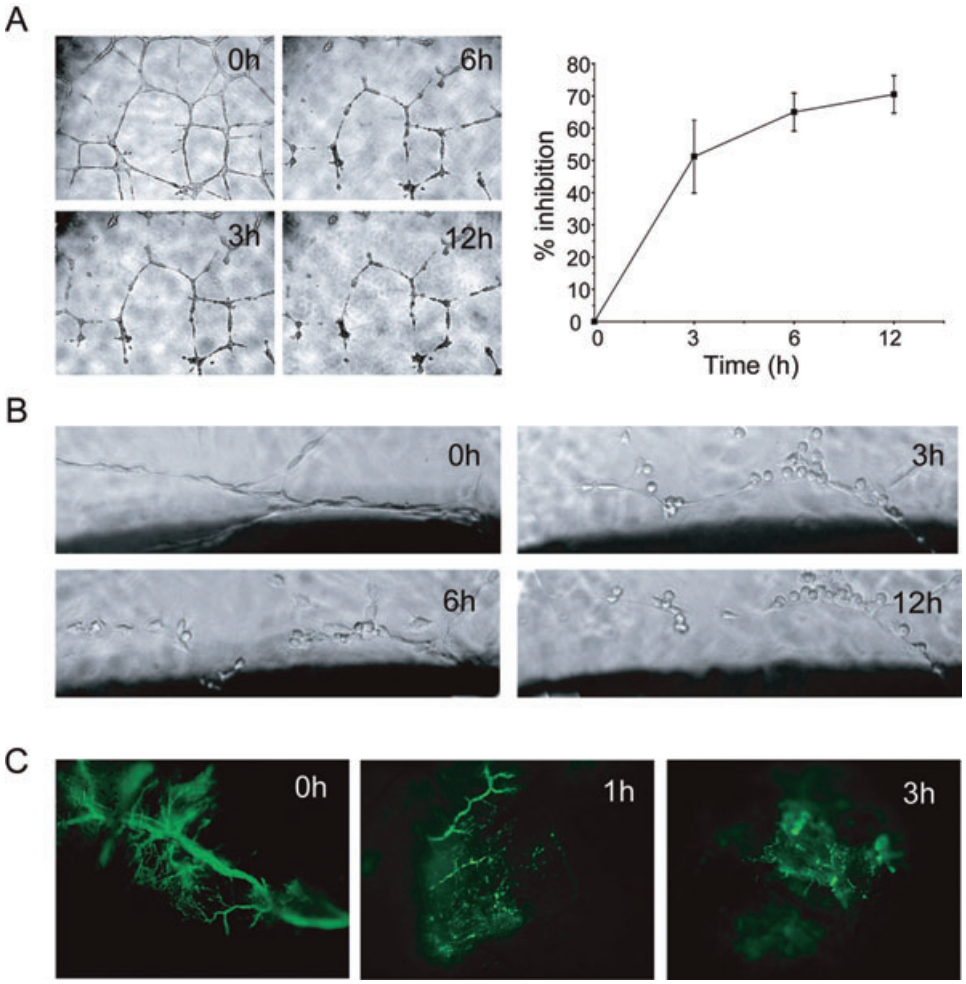

Figure 5 Vascular targeting activity of C9. (A) Neovasculature network disruption assay: cells were plated on Matrigel and allowed to form capillary-like networks for 24 h. These networks were then exposed to C9 (0.5 μmol·L^{-1}, 12 h). C9 treatment resulted in a time-dependent inhibition. Magnification, 100×. (B) Aortic ring assay; aortic rings were cultured for 7 days and then treated with C9 (0.5 μmol·L^{-1}) for 12 h. Magnification, 200×. (C) *In vivo* Matrigel plug assay. Fluorescence microscopy image of FITC-dextran perfusing the neovasculature before (0 h) and 1 and 3 h following C9 treatment (200 mg·kg^{-1}, i.p.), as described in *Methods*. The clearly visible blood vessels at 0 h were almost totally disrupted 3 h after i.p. injection of C9. Magnification, 200×.

tion, at non-toxic concentrations. All these suggested that the effect of C9 on the already formed vasculature and angiogenesis was related to its effects on endothelial cell function, rather than on cell proliferation.

Much ongoing research has attempted to elucidate the molecular bases of the anti-angiogenic and vascular targeting activity of microtubule-binding agents (Hotchkiss *et al*., 2002; Mabjeesh *et al*., 2003; Bijman *et al*., 2006), while it is widely accepted that the main effects of such agents result from their alteration of microtubule dynamics. In the present study, the inhibitory effects of C9 on microtubule dynamics and its affinity for tubulin have been clearly identified, as C9 disrupted the microtubule cytoskeleton through binding to tubulin via the colchicine site (but not the vinblastine-binding site). These results together indicated that impairment of microtubule function might be responsible for the anti-angiogenic or vascular targeting effects of C9. The attenuation of the effects of C9 by pretreatment with taxol, a microtubule-polymerizing agent, provides further support for this mechanism of action.

Evidence has suggested that Raf-MEK-ERK signalling molecules are required for angiogenesis (Gollob *et al*., 2006) and the microtubule inhibitors are known to elicit distinct and specific effects on mitogen-activated protein kinase-mediated signalling pathways (Tan *et al*., 2004). In our study, C9 decreased the activation of Raf-MEK-ERK signalling molecules stimulated by either VEGF or bFGF or FBS, but with no effects noted on phosphorylation of KDR or FGFR1. These results strongly suggested that the anti-angiogenic activities of C9 were partly mediated through the Raf-MEK-ERK1/2 signalling pathway.

Although the vascular targeting mechanisms have not, up to date, been clearly elucidated (Hotchkiss *et al*., 2002; Mabjeesh *et al*., 2003; Bijman *et al*., 2006), it has been suggested that changes in endothelial cell morphology are associated with vascular targeting activities, as cell contraction or retraction may cause an increase in vascular resistance and obstruction of tumour blood flow (Kanthou and Tozer, 2002). Such changes are critically regulated by the Rho/Rho kinase signalling pathway. In the current study, Y27632, a

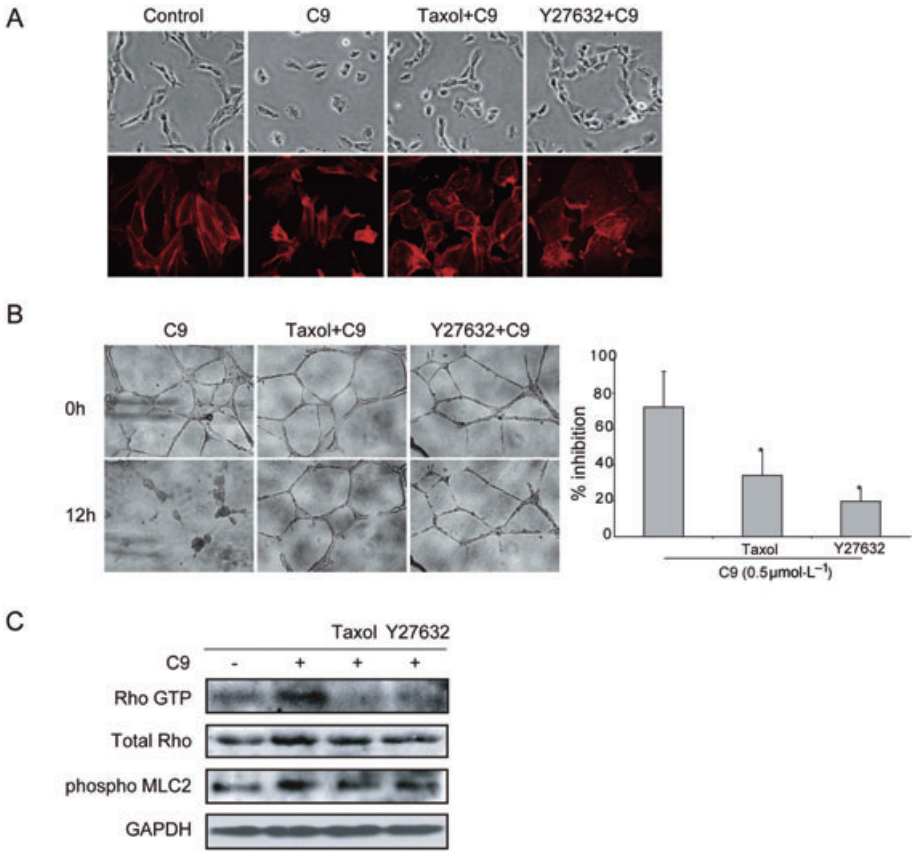

Figure 6 Microtubule disassembly contributed to the vascular disrupting activity of C9. (A) The change in endothelial cell morphology induced by C9 was attenuated by taxol and Y27632. Endothelial cells were pretreated with vehicle control (30 min), taxol (0.2 μmol·L^{-1}, 30 min) or Y27632 (10 μmol·L^{-1}, 30 min), then incubated with C9 (0.5 μmol·L^{-1}, 1 h). Cells were examined with an inverted microscope (40×) or stained for F-actin (red); fluorescence images were obtained by a fluorescence microscope (43×). (B) Effects of C9 on newly formed vessels were antagonized by taxol and Y27632. HUVECs were seeded onto Matrigel to form a functional network, then pretreated with or without taxol (0.2 μmol·L^{-1}, 30 min) or Y27632 (10 μmol·L^{-1}, 30 min) and then exposed to C9 (0.5 μmol·L^{-1}, 12 h); magnification, 100×. (C) C9 activated Rho GTPase and increased the phosphorylation of MLC2, which was antagonized by taxol and Y27632. Serum-starved HUVECs were treated with control or taxol (0.2 μmol·L^{-1}, 30 min) or Y27632 (10 μmol·L^{-1}, 30 min), prior to analysis of Rho activity. GAPDH, glyceraldehyde-3-phosphate dehydrogenase; HUVECs, human umbilical vein endothelial cells; MLC2, myosin light chain2.

Rho kinase inhibitor, attenuated cell morphology changes induced by C9. Similarly, pretreatment with Y27632 protected cord networks from disruption by C9. Consistent with the results of these morphological and immunofluorescence assays, C9 also activated Rho GTPase and the phosphorylation of MLC2, which was reversed by pretreatment with Y27632. All these findings suggest that C9 disrupted newly formed vessels via a Rho/Rho kinase pathway.

Crosstalk between the microtubule and the actin cytoskeleton is essential for the regulation of many cellular functions. Our findings that taxol reversed the effects of C9 on Rho GTPase and MLC2 phosphorylation indicated that the morphological and vascular disrupting activity of C9 was associated with the disruption of microtubules and actin reorganization. Taken together, these results suggested the C9 induced microtubule disassembly in endothelial cells and actin reorganization through the Rho/Rho kinase pathway; and it also suggested that its vascular disruption effect resulted from changes in endothelial cell morphology.

In conclusion, we demonstrated for the first time that C9, a newly synthesized microtubule-binding agent, exhibited both anti-angiogenic and vascular disrupting effects *in vivo* and *in vitro*. The Raf-MEK-ERK pathway and microtubule disruption were found to be associated with the anti-angiogenic activity of C9. Endothelial cell contraction and membrane blebbing involving the Rho/Rho kinase-dependent pathway were likely to be responsible for its vascular disrupting activity.

Acknowledgements

We thank Li-Juan Lu and Yong Xi for Matrigel plug assays and Dr Li Du for SPR-binding assays. This work was supported by grants from the national Natural Science Foundation of China (NSFC) (No. 30572201, No. 30721005 and No. 30730103).

Statement of conflict of interest

None.

References

Alley MC, Scudiero DA, Monks A, Hursey ML, Czerwinski MJ, Fine DL *et al.* (1988). Feasibility of drug screening with panels of human tumor cell lines using a microculture tetrazolium assay. *Cancer Res* **48**: 589–601.

Ashton AW, Yokota R, John G, Zhao S, Suadicani SO, Spray DC *et al.* (1999). Inhibition of endothelial cell migration, intercellular communication, and vascular tube formation by thromboxane A(2). *J Biol Chem* **274**: 35562–35570.

Belleri M, Ribatti D, Nicoli S, Cotelli F, Forti L, Vannini V *et al.* (2005). Antiangiogenic and vascular-targeting activity of the microtubule-destabilizing trans-resveratrol derivative 3,5,4′-trimethoxystilbene. *Mol Pharmacol* **67**: 1451–1459.

Bergers G, Javaherian K, Lo KM, Folkman J, Hanahan D (1999). Effects of angiogenesis inhibitors on multistage carcinogenesis in mice. *Science* **284**: 808–812.

Bergers G, Song S, Meyer-Morse N, Bergsland E, Hanahan D (2003). Benefits of targeting both pericytes and endothelial cells in the tumor vasculature with kinase inhibitors. *J Clin Invest* **111**: 1287–1295.

Bijman MN, van Nieuw Amerongen GP, Laurens N, van Hinsbergh VW, Boven E (2006). Microtubule-targeting agents inhibit angiogenesis at subtoxic concentrations, a process associated with inhibition of Rac1 and Cdc42 activity and changes in the endothelial cytoskeleton. *Mol Cancer Ther* **5**: 2348–2357.

Denekamp J (1993). Review article: angiogenesis neovascular proliferation and vascular pathophysiology as targets for cancer therapy. *Br J Radiol* **66**: 181–196.

Downing KH (2000). Structural basis for the interaction of tubulin with proteins and drugs that affect microtubule dynamics. *Annu Rev Cell Dev Biol* **16**: 89–111.

Ferrara N, Kerbel RS (2005). Angiogenesis as a therapeutic target. *Nature* **438**: 967–974.

Folkman J (1971). Tumor angiogenesis: therapeutic implications. *N Engl J Med* **285**: 1182–1186.

Folkman J (1995). Seminars in Medicine of the Beth Israel Hospital, Boston. Clinical applications of research on angiogenesis. *N Engl J Med* **333**: 1757–1763.

Folkman J (2007). Angiogenesis: an organizing principle for drug discovery? *Nat Rev Drug Discov* **6**: 273–286.

Gollob JA, Wilhelm S, Carter C, Kelley SL (2006). Role of Raf kinase in cancer: therapeutic potential of targeting the Raf/MEK/ERK signal transduction pathway. *Semin Oncol* **33**: 392–406.

Gupta K, Bishop J, Peck A, Brown J, Wilson L *et al.* (2004). Antimitotic antifungal compound benomyl inhibits brain microtubule polymerization and dynamics and cancer cell proliferation at mitosis, by binding to a novel site in tubulin. *Biochemistry* **43**: 6645–6655.

Hastie SB (1991). Interactions of colchicine with tubulin. *Pharmacol Ther* **51**: 377–401.

Hotchkiss KA, Ashton AW, Mahmood R, Russell RG, Sparano JA, Schwartz EL (2002). Inhibition of endothelial cell function in vitro and angiogenesis in vivo by docetaxel (Taxotere): association with impaired repositioning of the microtubule organizing center. *Mol Cancer Ther* **1**: 1191–1200.

Jaffe EA, Nachman RL, Becker CG, Minick CR (1973). Culture of human endothelial cells derived from umbilical veins. Identification by morphologic and immunologic criteria. *J Clin Invest* **52**: 2745–2756.

Jordan MA, Wilson L (1998). Microtubules and actin filaments: dynamic targets for cancer chemotherapy. *Curr Opin Cell Biol* **10**: 123–130.

Kanthou C, Tozer GM (2002). The tumor vascular targeting agent combretastatin A-4-phosphate induces reorganization of the actin cytoskeleton and early membrane blebbing in human endothelial cells. *Blood* **99**: 2060–2069.

Kruczynski A, Poli M, Dossi R, Chazottes E, Berrichon G, Ricome C *et al.* (2006). Anti-angiogenic, vascular-disrupting and anti-metastatic activities of vinflunine, the latest vinca alkaloid in clinical development. *Eur J Cancer* **42**: 2821–2832.

Landuyt W, Verdoes O, Darius DO, Drijkoningen M, Nuyts S, Theys J *et al.* (2000). Vascular targeting of solid tumours: a major 'inverse' volume-response relationship following combretastatin A-4 phosphate treatment of rat rhabdomyosarcomas. *Eur J Cancer* **36**: 1833–1843.

Li PK, Xiao Z, Hu Z, Pandit B, Sun Y, Sackett DL *et al.* (2005). Conformationally restricted analogs of Combretastatin A-4 derived from SU5416. *Bioorg Med Chem Lett* **15**: 5382–5385.

Li W, Shao Y, Hu L, Zhang X, Chen Y, Tong L *et al.* (2007). BM6, a new semi-synthetic vinca alkaloid, exhibits its potent in vivo anti-tumor activities via its high binding affinity for tubulin and improved pharmacokinetic profiles. *Cancer Biol Ther* **6** (5): 787–794.

Mabjeesh NJ, Escuin D, LaVallee TM, Pribluda VS, Swartz GM, Johnson MS *et al.* (2003). 2ME2 inhibits tumor growth and angiogenesis by disrupting microtubules and dysregulating HIF. *Cancer Cell* **3**: 363–375.

Micheletti G, Poli M, Borsotti P, Martinelli M, Imberti B, Taraboletti G *et al.* (2003). Vascular-targeting activity of ZD6126, a novel tubulin-binding agent. *Cancer Res* **63**: 1534–1537.

Neri D, Bicknell R (2005). Tumour vascular targeting. *Nat Rev Cancer* **5**: 436–446.

Nicosia RF, Ottinetti A (1990). Growth of microvessels in serum-free matrix culture of rat aorta. A quantitative assay of angiogenesis in vitro. *Lab Invest* **63**: 115–122.

Osusky KL, Hallahan DE, Fu A, Ye F, Shyr Y, Geng L (2004). The receptor tyrosine kinase inhibitor SU11248 impedes endothelial cell migration, tubule formation, and blood vessel formation in vivo, but has little effect on existing tumor vessels. *Angiogenesis* **7**: 225–233.

Pandit B, Sun Y, Chen P, Sackett DL, Hu Z, Rich W *et al.* (2006). Structure-activity-relationship studies of conformationally restricted analogs of combretastatin A-4 derived from SU5416. *Bioorg Med Chem* **14**: 6492–6501.

Ravelli RB, Gigant B, Curmi PA, Jourdain I, Lachkar S, Sobel A *et al.* (2004). Insight into tubulin regulation from a complex with colchicine and a stathmin-like domain. *Nature* **428**: 198–202.

Ren XD, Kiosses WB, Schwartz MA (1999). Regulation of the small GTP-binding protein Rho by cell adhesion and the cytoskeleton. *EMBO J* **18**: 578–585.

Ribatti D, Vacca A, Roncali L, Dammacco F (2000). The chick embryo chorioallantoic membrane as a model for in vivo research on anti-angiogenesis. *Curr Pharm Biotechnol* **1**: 73–82.

Schmidt A, Wenzel D, Thorey I, Sasaki T, Hescheler J, Timpl R *et al.* (2006). Endostatin influences endothelial morphology via the activated ERK1/2-kinase endothelial morphology and signal transduction. *Microvasc Res* **71**: 152–162.

Siemann DW, Rojiani AM (2005). The vascular disrupting agent ZD6126 shows increased antitumor efficacy and enhanced radiation response in large, advanced tumors. *Int J Radiat Oncol Biol Phys* **62**: 846–853.

Soeda S, Kozako T, Iwata K, Shimeno H (2000). Oversulfated fucoidan inhibits the basic fibroblast growth factor-induced tube formation by human umbilical vein endothelial cells: its possible mechanism of action. *Biochim Biophys Acta* **1497**: 127–134.

Tan WF, Zhang XW, Li MH, Yue JM, Chen Y, Lin LP *et al.* (2004). Pseudolarix acid B inhibits angiogenesis by antagonizing the vascular endothelial growth factor-mediated anti-apoptotic effect. *Eur J Pharmacol* **499**: 219–228.

Taraboletti G, Micheletti G, Dossi R, Borsotti P, Martinelli M, Fiordaliso F *et al*. (2005). Potential antagonism of tubulin-binding anticancer agents in combination therapies. *Clin Cancer Res* **11**: 2720–2726.

Thorpe PE (2004). Vascular targeting agents as cancer therapeutics. *Clin Cancer Res* **10**: 415–427.

Vincent L, Kermani P, Young LM, Cheng J, Zhang F, Shido K *et al*. (2005). Combretastatin A4 phosphate induces rapid regression of tumor neovessels and growth through interference with vascular endothelial-cadherin signaling. *J Clin Invest* **115**: 2992–3006.